

Environmental Photochemistry of Fenamate NSAIDs and their Radical Intermediates

Caroline A. Davis^{1,2}, Paul R. Erickson¹, Kristopher McNeill^{1*}, Elisabeth M.L. Janssen^{2*}

¹Institute of Biogeochemistry and Pollutant Dynamics, ETH Zurich, 8092 Zurich, Switzerland

²Department of Environmental Chemistry, Swiss Federal Institute of Aquatic Science and Technology (Eawag), 8600 Dübendorf, Switzerland

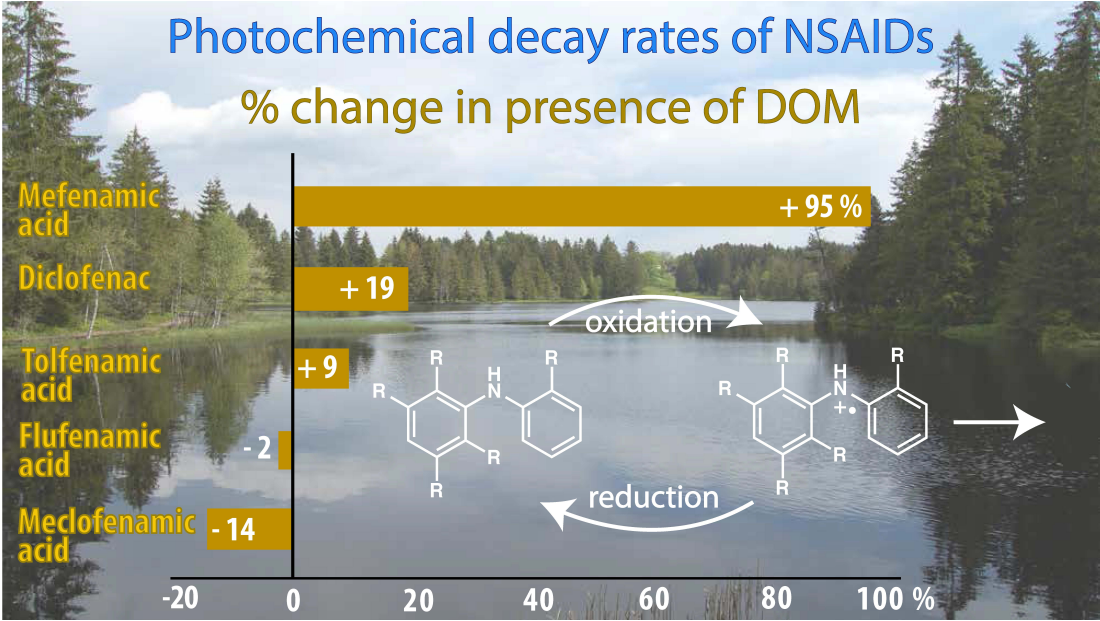
*Co-corresponding authors

E-mail: elisabeth.janssen@eawag.ch

Phone: + 41 58 765 5802

E-mail: kris.mcneill@env.ethz.ch

Phone: +41 44 632 3755



Abstract

Fenamates are a class of non-steroidal anti-inflammatory drugs (NSAIDs) that are not fully removed during wastewater treatment and can be released to surface waters. Here, near-surface photochemical half-lives were evaluated to range from minutes to hours of four fenamates and the closely related diclofenac. While quantum yields for direct photochemical reactions at the water surface vary widely from 0.071 for diclofenac to <0.001 for mefenamic acid, all fenamates showed significant reactivity towards singlet oxygen and hydroxyl radical with bimolecular reaction rate constants of $1.3\text{--}2.8 \times 10^7 \text{ M}^{-1}\text{s}^{-1}$ and $1.1\text{--}2.7 \times 10^{10} \text{ M}^{-1}\text{s}^{-1}$, respectively. Photodecay rates increased in the presence of dissolved organic matter (DOM) for diclofenac (+19%), tolfenamic acid (+9%), and mefenamic acid (+95%), but decreased for flufenamic acid (-2%) and meclofenamic acid (-14%) after accounting for light screening effects. Fast reaction rate constants of all NSAIDs with model triplet sensitizers were quantified by laser flash photolysis. Here, the direct observation of diphenylamine radical intermediates by transient absorption spectroscopy demonstrates one-electron oxidation of all fenamates. Quenching rate constants of these radical intermediates by ascorbic acid, a model antioxidant, were also quantified. These observations suggest that the balance of oxidation by photoexcited triplet DOM and quenching of the formed radical intermediates by antioxidant moieties determines whether net sensitization or net quenching by DOM occurs in the photochemical degradation of fenamates.

Keywords: pharmaceuticals, transformation, antioxidant, diclofenac, diphenylamine

Introduction

Fenamates are nonsteroidal anti-inflammatory drugs (NSAIDs) that contain fenamic acid (N-phenylanthranilic acid) as a core structural unit (Figure 1). Members of this family include mefenamic acid, flufenamic acid, meclofenamic acid, and tolafenamic acid. Diclofenac is closely related, having a methylene (CH_2) separating the diphenylamine substructure from the acid moiety. The therapeutic effect of pain relief is achieved by inhibiting cyclooxygenase enzymes, which facilitate the oxidation of arachidonic acid and initiate the downstream inflammation response in mammals, including humans.¹⁻⁴ Fenamate-based NSAIDs are excreted by humans and animals⁵⁻⁸, are not always completely removed during wastewater treatment, and thus, high effluent concentrations can contribute to entry of these drugs into surface waters.⁹⁻¹²

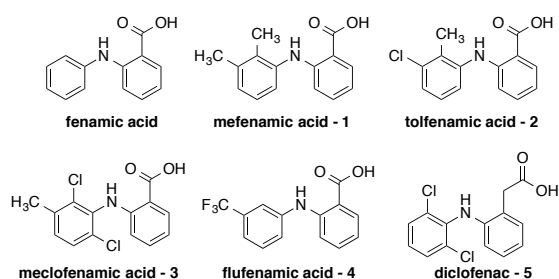


Figure 1. Structures of fenamic acid and the fenamate NSAIDs mefenamic acid - 1, tolafenamic acid - 2, meclofenamic acid - 3, and flufenamic acid - 4, and diclofenac - 5.

Mefenamic acid, marketed worldwide as Ponstel or Ponstan, has been detected in wastewater effluents at concentrations up to $1.4 \mu\text{g L}^{-1}$ in Switzerland¹³ and up to $0.14 \mu\text{g L}^{-1}$ in Chinese surface waters.¹⁴ Flufenamic acid (Flufen, Opyrin) a trifluoromethylated fenamate, is only sold in a limited number of countries, but was also detected in Spanish wastewater influent and effluent.¹⁵ Other fenamate drugs, meclofenamic acid (Meclomen, Eucome) and tolafenamic acid (Clotam, Tolfedine) contain chloro and methyl groups, are primarily used in veterinary medicine, and are sold mostly in Asia and limited parts of Europe. So far, insufficient information is available about their concentration in surface waters because these fenamates have rarely been included in environmental screening studies. Few studies show that their concentrations were below the limit of detection ($0.050 \mu\text{g L}^{-1}$)^{16,17}, however, tolafenamic acid had been detected at up to $1.6 \mu\text{g L}^{-1}$ in Brazilian wastewater treatment plant effluents.¹⁸ Diclofenac, which is sold under various trade names such

as Arthrotec, Cataflam, and Voltaren, is one of the most abundantly sold NSAIDs worldwide¹⁹ and has been implicated in the mass killing of Asian vultures.²⁰ Consequently, diclofenac has been more extensively studied and has been detected in microgram per liter concentrations in various wastewater treatment plant influents and effluents^{13, 16, 17, 21-26} as well as in surface waters^{16, 18, 27}, and studies demonstrate no significant biodegradation.^{28,29} While diclofenac is routinely monitored and wastewater treatment aims to limit its discharge into surface waters, less attention has been given to fenamates. These pharmaceuticals exhibit the same mode of action (NSAIDs, inhibiting cyclooxygenases) and the co-occurrence of these drugs may lead to synergistic effects in the environment.

All fenamates have pK_a values ranging from 3.7 to 4.3^{7, 30-33}, making them ionic at neutral pH. The estimated octanol-water partitioning coefficients for the ionic species, $\log D_{ow}$, range from 2 to 3 (Table S1 in the electronic supplementary information, ESI), and was experimentally determined as 0.68 for diclofenac³⁴ and as 1.6 for mefenamic acid.³⁵ These parameters suggest that sorption and sedimentation are not the most important pathways for removal of such compounds from the aqueous phase.

Once in surface waters, photochemical transformation processes may be some of the most relevant removal pathways of fenamates. Several previous studies focused on the direct photochemical transformation of diclofenac and estimated an environmental half-life in sunlight between 30 minutes to 1 hour in the top layer of a water column^{21, 36}, which is affected in natural water due to light screening by dissolved organic matter (DOM).²³ The photochemical half-lives of fenamates have only been partially investigated, e.g., for flufenamic acid (1 hour, artificial light: 300-450 nm)³⁷ and for mefenamic acid (33 hours, noon sunlight, 45° N latitude).³⁸ So far the indirect photochemical pathways, including transformation by reactive oxygen species or interactions with DOM for have not been studied in detail for these fenamates.

This study presents a detailed investigation of the environmental photochemical transformation kinetics and mechanisms of the fenamates and diclofenac by comparing direct and indirect photochemical degradation processes. While direct photodegradation dominates for some of the compounds at the water surface, the results demonstrate that reactions with reactive oxygen species and photochemically

excited DOM are significant, especially deeper in the water column. In particular, the interactions with DOM as a natural photochemical sensitizer and antioxidant towards radical intermediates were directly observed and quantified by transient absorption spectroscopy.

Material and Methods

Materials. Experiments were carried out buffer from potassium phosphate dibasic (Sigma-Aldrich, $\geq 98\%$) and potassium dihydrogen phosphate (Fluka, $\geq 99.5\%$). Aqueous solutions were prepared with ultrapure water ($>18\text{ M}\Omega\text{ cm}$, Barnstead Nanopure Diamond system). The following reagents were all purchased from Sigma-Aldrich and used as received: acetonitrile (HPLC grade), methanol (HPLC grade), 2-hydroxyterephthalic acid (97%), L(+)-ascorbic acid sodium salt ($\geq 99.5\%$), caffeic acid ($\geq 98\%$), diclofenac sodium salt (≥ 98.5), lumichrome, meclofenamic acid sodium salt, perinaphthenone (97%), pyridine (Chromosolv $\geq 99.9\%$), Rose Bengal (95%), sodium acetate trihydrate ($\geq 99.0\%$), sodium benzoate (BioUltra $\geq 99.5\%$), sodium nitrite ($\geq 99\%$) and tolfenamic acid. Flufenamic acid (97%) was purchased from Acros Organics. 4-nitroanisole (Sigma-Aldrich, 97%) was recrystallized before use. The dipotassium terephthalate salt (K_2TPA) was prepared from terephthalic acid (Sigma-Aldrich, 98%) as described elsewhere³⁹. Acetic acid ($\geq 99.8\%$), hydrogen peroxide (Trace Select $\geq 30\%$, no stabilizers), mefenamic acid ($\geq 98\%$), and sodium azide ($\geq 99.0\%$) were obtained from Fluka. Sodium molybdate dihydrate ($\geq 99.5\%$) was purchased from Merck. Furfuryl alcohol (Merck, $\geq 98\%$) was distilled prior to use and kept under argon to prevent oxidation. Deuterium oxide (99.8 atom% D) was purchased from Armar Isotopes. Pony Lake Fulvic Acid (1R109F) and Suwannee River Fulvic Acid (2S101F) were purchased from the International Humic Substance Society (IHSS).

Methods. All light exposure tests were performed with 5 μ M test compounds (**1-5**) in phosphate buffer (5 μ M, pH 7.5) and dark controls were included, unless stated otherwise.

Simulated Sunlight Exposure. Compounds **1-5** were individually exposed to simulated sunlight (Heraeus model Suntest CPS+) in open quartz test tubes, positioned at a 20° angle from the horizontal plane, 30 cm below the light source, and submerged in a temperature-controlled water bath (27°C \pm 1°C). Furfuryl alcohol (FFA, 40 μ M) was used for quantification of singlet oxygen. Additional samples were prepared containing the humic substance isolate Pony Lake Fulvic Acid (PLFA, 10 mg carbon L⁻¹). Aliquots were taken in triplicates and analyzed for the test compound and FFA as described below. To calculate the quantum yield of direct photochemical reactions, the chemical actinometer system PNA-PYR (10 μ M p-nitroanisole, 0.5 mM pyridine) were irradiated with simulated sunlight in nanopure water in identical test tubes alongside the test compounds. The quantum yields for the test compounds, $\phi_{\text{test comp.}}$, are expressed as:

$$\phi_{\text{test comp.}} = \phi_{\text{act.}} \cdot \left(\frac{k_{\text{test comp.}}}{k_{\text{act.}}} \right) \cdot \left(\frac{\sum_{\lambda} \epsilon_{\lambda, \text{act.}} \cdot L_{\lambda, \text{rel.}}}{\sum_{\lambda} \epsilon_{\lambda, \text{test comp.}} \cdot L_{\lambda, \text{rel.}}} \right) \quad (1)$$

with the observed degradation rate constants k (s⁻¹), the quantum yield of the actinometer $\phi_{\text{act.}}$ being 0.29[PYR] + 0.00029⁴⁰, the wavelength dependent molar absorptivities ϵ , and relative light irradiance of the simulated sunlight.⁴¹

Reactivity with Singlet Oxygen. To determine the bimolecular reaction rate constants of compounds **1-5** with singlet oxygen, ¹O₂, four different methods have been evaluated. The methods include photochemically sensitized experiments with Rose Bengal, time-resolved ¹O₂ phosphorescence quenching, non-photochemical

generation of $^1\text{O}_2$ by hydrogen peroxide and molybdate, and finally the evaluation of the kinetic solvent isotope effect (KSIE) in D_2O .^{42,43} The former three methods may produce artifacts due to high reactivity of the test compounds with triplet excited dyes, contribution of physical quenching, and instability at high solution pH required, respectively. Thus, the KSIE method was chosen to determine the reaction rate constants. Details about these methods can be found in the ESI (Text S1 and Figure S1). The KSIE method depends on an increase in $^1\text{O}_2$ lifetime in D_2O that is reflected by a higher $^1\text{O}_2$ steady-state concentration, $[^1\text{O}_2]_{\text{ss}}$. Faster degradation of compounds **1-5** in D_2O can be quantitatively attributed to the reaction with $^1\text{O}_2$. For the KSIE tests, samples were prepared with 5 μM compounds **1-5**, 0.77 μM perinaphthenone, and 40 μM FFA as the $^1\text{O}_2$ probe in either H_2O or approximately 90% D_2O at pH 7.5 (phosphate buffer, 5 mM, Text S2 and Table S2). Samples were irradiated in open borosilicate test tubes with enhanced UVA light (2 bulbs, centered at 365 nm) on a turn table in a Rayonet photoreactor (Southern New England Ultraviolet Company, Branford, USA) with a polymer heat/bandpass filter situated between the lamps and the samples to remove light below 320 nm (269 LEE Heat Shield, Lee Filters, Hampshire, UK), in addition to long wavelengths (> 400 nm). The bimolecular reaction rate constant with $^1\text{O}_2$, $k_{\text{rxn},^1\text{O}_2}$, was estimated as:

$$k_{\text{rxn},^1\text{O}_2} = \frac{k_{\text{D}_2\text{O}} - k_{\text{H}_2\text{O}}}{[^1\text{O}_2]_{\text{ss},\text{D}_2\text{O}} - [^1\text{O}_2]_{\text{ss},\text{H}_2\text{O}}} \quad (2)$$

with the observed decay rate constants in D_2O ($k_{\text{D}_2\text{O}}$) and in H_2O ($k_{\text{H}_2\text{O}}$) and the respective steady-state concentrations of $^1\text{O}_2$, $[^1\text{O}_2]_{\text{ss}}$ calculated from the observed decay rates of FFA at 23°C with a known reaction rate constant of $1.03 \pm 0.01 \times 10^8 \text{ M}^{-1}\text{s}^{-1}$ (specific for this temperature) as detailed in Text S3.⁴²

Reactivity with Hydroxyl Radical. The bimolecular reaction rate constants with hydroxyl radical, $\bullet\text{OH}$, were determined using benzoic acid as a reference compound. Samples were prepared with 10 μM sodium benzoate, and 1 mM H_2O_2 and were irradiated in a Rayonet photoreactor with enhanced UVA light (emission centered at 365 nm, 8 bulbs). Sodium nitrite (6.5 μM) was used as a $\bullet\text{OH}$ source for meclofenamic acid because not enough $\bullet\text{OH}$ were produced from H_2O_2 to distinguish

decay due to $\bullet\text{OH}$ vs. direct photochemical decay. Control samples without H_2O_2 (or nitrite) were also tested. Competition plots were generated by plotting the normalized decay of test compounds, $\ln(C/C_0)$ against that of benzoic acid and the slope, S , was determined by linear regression. The bimolecular reaction rate constant of test compounds was assessed as:

$$k_{rxn,\bullet OH} = S \cdot k_{rxn(BZA)} \quad (3)$$

with $k_{rxn(BZA)}$ being the bimolecular reaction rate constant of benzoic acid ($5.9 \pm 0.1 \times 10^9 \text{ M}^{-1} \text{ s}^{-1}$).⁴⁴ The steady-state concentration of $\bullet\text{OH}$, $[\bullet\text{OH}]_{ss}$, produced by DOM ($10 \text{ mg}_c \text{ L}^{-1}$ PLFA) in the solar simulator was quantified using terephthalic acid (TPA, $10 \mu\text{M}$) as the $\bullet\text{OH}$ probe by monitoring the formation of hydroxylated product 2-hydroxyterephthalic acid (hTPA).

Reactivity with Triplet Sensitizer and Antioxidants. To determine the reactivity of compounds **1-5** with photochemically excited triplet sensitizers, perinaphthenone was used as a model sensitizer. Samples contained $0.77 \mu\text{M}$ of perinaphthenone and were irradiated in open borosilicate test tubes with enhanced UVA light (2 bulbs, with heat/bandpass filter) on a turn table in a Rayonet photoreactor. Additional experiments were conducted with identical samples, but sealed and sparged with argon for 15 minutes prior to irradiation to remove O_2 , an effective triplet quencher. Control samples without perinaphthenone were also included. Additional tests were performed in the presence of a model antioxidant, $10 \mu\text{M}$ caffeic acid (3,4-dihydroxycinnamic acid). Caffeic acid represents a plant-derived diphenoxy-based reducing agent with relatively low absorbance of UVA light, which minimizes its direct photodecay in these tests.

Sample Analysis. Samples were analyzed for compounds **1-5** by Ultra Performance Liquid Chromatography (UPLC) on a C18 column (Waters Acquity, BEH 130 C18, $1.7 \mu\text{m}$, $2.1 \times 150 \text{ mm}$), injection volume of $5 \mu\text{L}$, 0.20 ml min^{-1} flow rate with an isocratic method of eluent (A) 0.1% formic acid with 10% acetonitrile and (B) 100% acetonitrile at a ratio of 20:80 (A:B) and detection by absorbance at 288 nm. Benzoic acid was analyzed with an eluent ratio of 70:30 (A:B) by absorbance detection at

245 nm. 2-hydroxyterephthalic acid was analyzed with an eluent composition of (A) 0.1% formic acid with 10% methanol (MeOH) and (B) 100% MeOH at 70:30 (A:B) and detection by fluorescence (excitation: 250 nm, emission: 410 nm). Furfuryl alcohol and p-nitroanisole were analyzed on a C18 column (Agilent Eclipse - XDB C18, 5 μ m, 4.6 \times 150 mm) at 1.0 ml min⁻¹ flow rate with an eluent composition of (A) sodium acetate buffer (pH 5.9, 15.6 mM) and (B) 100% acetonitrile isocratically at a ratio of 90:10 and 40:60 (A:B), respectively and were detected by absorbance at 219 nm and 316 nm, respectively. All first-order degradation rate constants, k_{obs} (s⁻¹), were assessed as the slope of a linear regression of natural log-transformed normalized concentration, $\ln(C/C_0)$, versus irradiation time.

Transient Absorption Spectroscopy. To further elucidate the reaction mechanisms of compounds **1-5** with triplet excited states, laser flash photolysis was used to (a) determine reaction rate constants with triplet sensitizer, (b) evaluate the formation of radical intermediates, and (c) quantify the reactivity of these radical intermediates with antioxidants. Perinaphthenone (PN) and lumichrome were chosen as model sensitizers and ascorbic acid as a model antioxidant. Perinaphthenone was selected because of literature precedent³⁸ and because it is a conservative representative model sensitizer for CDOM due to its relatively low triplet energy ($E_T = 164 \text{ kJ mol}^{-1}$) and triplet state one-electron reduction potential ($E^{o*} (^3S^*/S^-) = 1.03 \text{ V}_{\text{SHE}}$).⁴⁵ Lumichrome was selected to generate fenamate radical intermediates in the laser system due to its higher reduction potential ($E^{o*} (^3S^*/S^-) = 1.91 \text{ V}_{\text{SHE}}$).⁴⁵ Both sensitizers were also suitable for laser experiments because their triplet signals did not overlap with the transient signals from the fenamates. Ascorbic acid was selected as a model antioxidant because of its high Trolox equivalent antioxidant capacity (1.03 $\text{TEAC}_{\text{ABTS}}^*$)⁴⁶ and also because its absorption spectrum did not overlap with the excitation wavelengths used for the laser experiments.

Transient absorption spectroscopy was carried out using a pump-probe system (EOS, Ultrafast Systems, Sarasota, USA). Pump pulses were produced by a regeneratively amplified Ti:sapphire laser, (output of 3.5 W at 795 nm, 1 kHz Solstice, Newport Spectra-Physics, Irvine, USA), which were converted to the desired excitation wavelength of 365 nm using a TOPAS Optical Parametric Amplifier (Light Conversion, Vilnius, Lithuania). Samples contained 100 μ M

perinaphthenone and increasing concentrations of compounds **1-5** (100-1000 μM) in 50% acetonitrile continuously sparged with synthetic air. The time-dependent change in absorbance (ΔA) for the triplet-excited state feature ($^3\text{PN}^*$, centered at 490 nm) was monitored. Transient absorbance traces were fit to exponential decay functions for lifetime estimates, τ ($= 1/k_{\text{obs}}$) (OriginPro 9.0, OriginLab Corp. Northampton, MA). The bimolecular reaction rate constants, $k(^3\text{PN}^*)$, of test compounds with the triplet sensitizer were obtained from the slope of linear regression of measured triplet decay rate constants, $k_{\text{obs}}(^3\text{PN}^*)$, versus concentration of compounds **1-5** (Figure S2-5). The quenching rate constant of $^3\text{PN}^*$ by the antioxidant, caffeic acid was also assessed in this manner (Figure S6).

To evaluate the formation of radical intermediates of the test compounds upon reaction with triplet sensitizer, further experiments were performed with lumichrome (100 μM , excitation at 370 nm), 400 μM compounds **1-5**, in phosphate buffer at pH 6.0 with 50% acetonitrile, sparged continuously with argon. Transient absorbance spectra were evaluated for radical intermediates of compounds **1-5**.

Lastly, to evaluate the reactivity of the radical intermediates with antioxidants, the change of τ of radical intermediates was measured in the presence of increasing concentrations of ascorbic acid (100-1000 μM). The bimolecular reaction rate constant was assessed as the slope of the linear regression of the measured radical decay rate constants plotted versus concentration of ascorbic acid (Figure S7-9).

Results and Discussion

Photodegradation in Simulated Sunlight. The photochemical half-lives in surface waters of the pharmaceuticals were evaluated by exposing aqueous solutions to simulated sunlight in the absence and presence of DOM (PLFA, 10 $\text{mg}_\text{C} \text{ L}^{-1}$). Compounds **1-5** were irradiated individually. Data in Figure 2 show that the pseudo-first-order decay rates in the presence of DOM were substantial for compounds **1-5**, but also varied significantly. In the presence of DOM, diclofenac was degraded the fastest ($t_{1/2} = 19$ min), followed by flufenamic acid, meclofenamic acid, tolfenamic

300 acid, and mefenamic acid ($t_{1/2}$ = 9.4 hours). The same order was observed in the
301 absence of DOM (Figure S10).

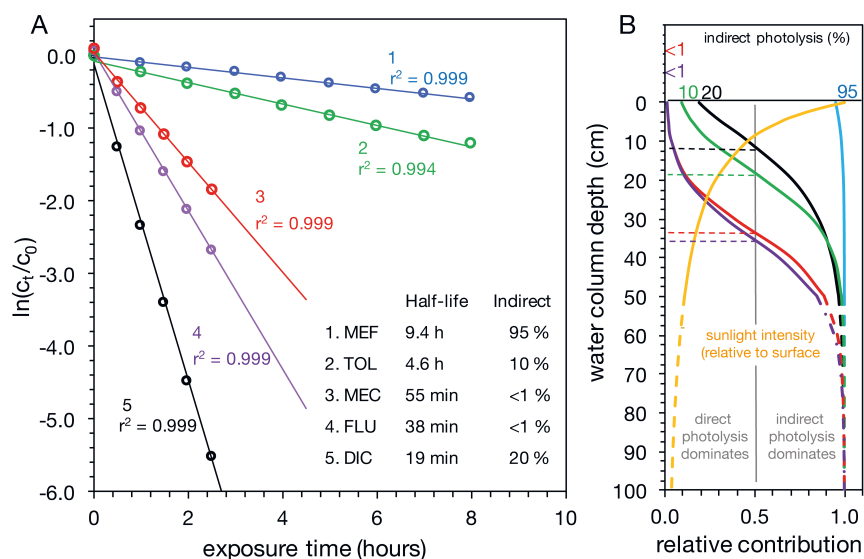


Figure 2. (A) Degradation kinetic plots of the fenamate drugs in the solar simulator in solution with Pony Lake Fulvic Acid (PLFA, 10 mg L⁻¹), buffered at pH 7.5, for mefenamic acid (1, blue), tolafenamic acid (2, green), meclofenamic acid (3, red), flufenamic acid (4, purple), and diclofenac (5, black). The table inset shows the half-lives under experimental conditions and the contribution of indirect photochemical reactions to the overall photodegradation. (B) Model of relative contribution of indirect photodecay to the overall photodegradation along the water column, and sunlight intensity (cumulative from 290-400 nm) for solar conditions in Zurich, Switzerland (47.3° N, mid-July) in the presence of dissolved organic matter (PLFA, 10 mg L⁻¹).

Quantum yields for direct photochemical transformation ranged from < 0.001 for mefenamic acid to 0.071 for diclofenac (Table 1). Flufenamic acid has a slightly lower quantum yield than meclofenamic acid, but its higher molar absorptivity across the solar spectrum results in an overall faster direct photochemical decay (Figure S11).

Not only the overall rates, but also the contribution of direct and indirect photochemical processes varied significantly among compounds **1-5**. The direct

photochemical degradation was compared to the overall degradation in the presence of DOM after accounting for light screening effects (Text S5 and Table S3). The decay rate constant increased for tolfenamic acid, diclofenac and mefenamic acid in the presence of DOM, with 9%, 20%, and 95% of the overall photodegradation being attributed to indirect photochemical processes, respectively. The relative indirect contribution for mefenamic acid is so high due to its negligible direct photochemical decay. DOM acted as a net sensitizer towards these compounds. The observed degradation rates of flufenamic acid and meclofenamic acid decreased in the presence of DOM by 2% and 14% respectively, even after accounting for light screening effects. Thus, DOM acted as a net quencher towards these two fenamates.

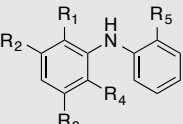
Data in Figure 2B show modeled contributions of indirect photochemical processes in a water column (model description in Text S6, Figure S11-S12). The sunlight intensity decreases with depth because chromophoric components (e.g., DOM) absorb light and particularly shorter wavelengths in the UV range do not penetrate deep into the water column.⁴⁸ Thus, all photochemical decay processes rapidly decrease down the water column where less light is available. Even though direct photochemical reactions dominated for compounds **2-5** at the water surface (top 1 cm), the relative contribution of indirect photochemical processes becomes competitive below the top 10-40 cm (Figure 2B).

First, indirect photochemical processes including reactions with singlet oxygen, hydroxyl radicals, and triplet excited sensitizers were quantified to evaluate the net sensitizing effect of DOM. Then the role of model antioxidants towards the photochemistry of fenamates and diclofenac was investigated to demonstrate the underlying mechanism of net quenching effects of DOM.

Role of Reactive Oxygen Species

Reactions with singlet oxygen ($^1\text{O}_2$) and hydroxyl radical ($\bullet\text{OH}$) can significantly contribute to the fate of some pollutants in surface waters. Thus far, the reaction rate constants of $^1\text{O}_2$ with compounds **1-5** had not been determined and only some rate constants existed for $\bullet\text{OH}$.

Table 1. Net effect of DOM, quantum yields for direct photochemical reactions, reaction rate constants with singlet oxygen $k(^1\text{O}_2)$, hydroxyl radical $k(\bullet\text{OH})$, model triplet sensitizer (perinaphthenone, $k(^3\text{PN}^*)$) for test compounds, and quenching rate constants of the radical intermediates of the test compounds with model antioxidant (ascorbic acid, $k(\text{AA})$).

Compound		Effect of DOM	Quantum yield	Reaction Rate Constants			
		Δk_{obs} (%)		$k(^1\text{O}_2)^a$ \pm std. dev. $\times 10^7$ ($\text{M}^{-1} \text{s}^{-1}$)	$k(\bullet\text{OH})$ \pm std. dev. $\times 10^{10}$ ($\text{M}^{-1} \text{s}^{-1}$)	$k(^3\text{PN}^*)$ \pm std. dev. $\times 10^8$ ($\text{M}^{-1} \text{s}^{-1}$)	$k(\text{AA})$ \pm std. dev. $\times 10^7$ ($\text{M}^{-1} \text{s}^{-1}$)
(1) Mefenamic acid	$\text{R}_1, \text{R}_2 = \text{CH}_3$ $\text{R}_3, \text{R}_4 = \text{H}$ $\text{R}_5 = \text{CO}_2^-$	+ 95 \pm 3	< 0.001	1.6 ± 0.7	1.1^c ± 0.2	20.0 ± 1.0	62.0 ± 3.0
(2) Tolfenamic acid	$\text{R}_1 = \text{CH}_3$, $\text{R}_2 = \text{Cl}$ R_3 , $\text{R}_4 = \text{H}$ $\text{R}_5 = \text{CO}_2^-$	+ 9 \pm 3	0.001	1.3 ± 0.6	1.3 ± 0.4	8.9 ± 1.3	21.0 ± 1.0
(3) Meclofenamic acid	$\text{R}_1, \text{R}_4 = \text{Cl}$ $\text{R}_2 = \text{H}$, $\text{R}_3 =$ CH_3 $\text{R}_5 = \text{CO}_2^-$	- 14 \pm 2	0.010	2.8 ± 0.6	2.8 ± 0.2	12.0 ± 2.0	3.3 ± 0.6
(4) Flufenamic acid	$\text{R}_1, \text{R}_2, \text{R}_4 = \text{H}$ $\text{R}_3 = \text{CF}_3$ $\text{R}_5 = \text{CO}_2^-$	- 2 \pm 1	0.006	1.3 ± 0.2	1.1^d ± 0.1	5.7 ± 0.5	6.9 ± 1.3
(5) Diclofenac (2-phenylacetic)	$\text{R}_1, \text{R}_4 = \text{Cl}$ $\text{R}_2, \text{R}_3 = \text{H}$ $\text{R}_5 = \text{CH}_2\text{CO}_2^-$	+ 19 \pm 2	0.071	n.d. ^b	1.6^e ± 0.1	4.2 ± 0.9	n.d. ^f

^adetermined by kinetic solvent isotope effect (Figure S13); ^bno significant rate constant detected with any of the applied methods (Figure S1 and S13); ^ccompare to $2.10 \times 10^{10} \text{ M}^{-1} \text{s}^{-1}$ by Aruoma et al.⁴⁹; ^dcompare to $1.30 \times 10^{10} \text{ M}^{-1} \text{s}^{-1}$ by Aruoma et al.⁴⁹; ^ecompare to $7.50 \times 10^9 \text{ M}^{-1} \text{s}^{-1}$ by Huber et al.⁵⁰; ^fno reaction rate constant was calculated because the radical intermediate of diclofenac was not detected under these conditions.

359

360 The bimolecular reaction rate constants of compounds **1-5** with $^1\text{O}_2$ were obtained
361 by rate comparison in H_2O versus D_2O (KSIE) and range from 1.3 to $2.8 \times 10^7 \text{ M}^{-1}\text{s}^{-1}$
362 (Table 1). All fenamates react significantly with $^1\text{O}_2$ when compared to other
363 pharmaceuticals for which reaction with $^1\text{O}_2$ was identified as a major decay process,
364 for example ranitidine ($1.6 \times 10^7 \text{ M}^{-1}\text{s}^{-1}$, pH 6.4)⁵¹, cimetidine ($9.2 \times 10^7 \text{ M}^{-1}\text{s}^{-1}$, pH
365 6.9)⁵¹ or sulfathiazole ($5.5 \times 10^7 \text{ M}^{-1}\text{s}^{-1}$)⁵². No significant KSIE was observed for
366 diclofenac and also in the $^1\text{O}_2$ phosphorescence experiments, increasing
367 concentrations of diclofenac did not show measurable quenching of $^1\text{O}_2$.

368 The measured reaction rate constants with $^1\text{O}_2$ ($k_{\text{rxn},^1\text{O}_2}$) allow estimation of the
369 relative contribution via reaction with $^1\text{O}_2$ to the overall photodegradation (Table S4).
370 Therefore, $k_{\text{rxn},^1\text{O}_2}$ was multiplied by the steady-state concentrations of $^1\text{O}_2$ ranging
371 from 2.9 - $3.3 \times 10^{-13} \text{ M}$ under simulated sunlight conditions (Figure 2A). The reaction
372 pathway with $^1\text{O}_2$ was most important for mefenamic acid, with 24% of its total
373 observed degradation in the presence of DOM. Tolfenamic, meclofenamic, and
374 flufenamic acid had a lower contribution of reaction with $^1\text{O}_2$ of 10%, 4% and 1% of
375 the total degradation, respectively.

376 The bimolecular reaction rate constants of compounds **1-5** with $\bullet\text{OH}$, $k_{\text{rxn},\bullet\text{OH}}$, was
377 obtained by competition experiments with benzoic acid and photochemical $\bullet\text{OH}$
378 generation (Figure S14). The reaction with $\bullet\text{OH}$ is rather unspecific and occurs at
379 nearly diffusion controlled rates for compounds **1-5** ranging from 1.0 to $2.7 \times 10^{10} \text{ M}^{-1}\text{s}^{-1}$.
380 Analogous to the pathway with $^1\text{O}_2$, the contribution to the overall
381 photodegradation via reaction with $\bullet\text{OH}$ under simulated sunlight conditions (Figure
382 2A) was determined by multiplying $k_{\text{rxn},\bullet\text{OH}}$ with the steady-state concentration of $\bullet\text{OH}$.
383 Despite the high reactivity with $\bullet\text{OH}$, the overall contributions for compounds **1-5**

range only from 0.1-1.3% (Table S4) because of the low steady-state concentration of $\bullet\text{OH}$ of $2.4 \times 10^{-17} \text{ M}$.

Role of Triplet Sensitizing and Antioxidant Moieties in DOM

Dissolved organic matter is redox active and can act as both a sensitizer and an antioxidant. Consequently, DOM can decrease or increase photochemical half-lives of organic molecules. Here, mefenamic acid, tolfenamic acid, and diclofenac underwent enhanced photochemical degradation in the presence of DOM with contribution of 95%, 9% and 20% to the overall decay rate constant, k_{obs} , respectively (Table 1). A summary of the contribution of reaction with $^1\text{O}_2$ and $\bullet\text{OH}$ to the overall indirect photodegradation can be found in Table S4. For tolfenamic acid, the 9% enhancement of photodegradation is seemingly explained by the reaction with $^1\text{O}_2$ (approx. 10%). For mefenamic acid and diclofenac however, a remaining 71% and 20% of the enhanced degradation, respectively, cannot be explained by the presence of reactive oxygen species alone (i.e., $^1\text{O}_2$ and $\bullet\text{OH}$) and must come from additional reaction pathways. In contrast, the presence of DOM reduced the photochemical half-lives of meclofenamic acid and flufenamic acid by 14% and 2%, respectively.

The reaction mechanisms behind the dual roles of DOM as sensitizer and quenchers were investigated further by employing model triplet sensitizers and model antioxidants. Data in Figure 3A show the pseudo-first order decay curves for diclofenac during irradiation with UVA light, minimizing the influence of direct photochemical processes. Photodegradation was enhanced in the presence of the photosensitizers with further enhancement under anoxic conditions. Oxygen is a strong triplet quencher and its removal increases triplet steady-state concentration. Consequently, a compound reactive towards triplets would decay faster under anoxic

conditions. Previous photochemical studies with mefenamic acid also revealed increased photodegradation in the presence of a model photosensitizer, perinaphthenone, particularly under anoxic conditions.³⁸ Here, the same trends were verified for all fenamates and diclofenac (Figure S15-S18).

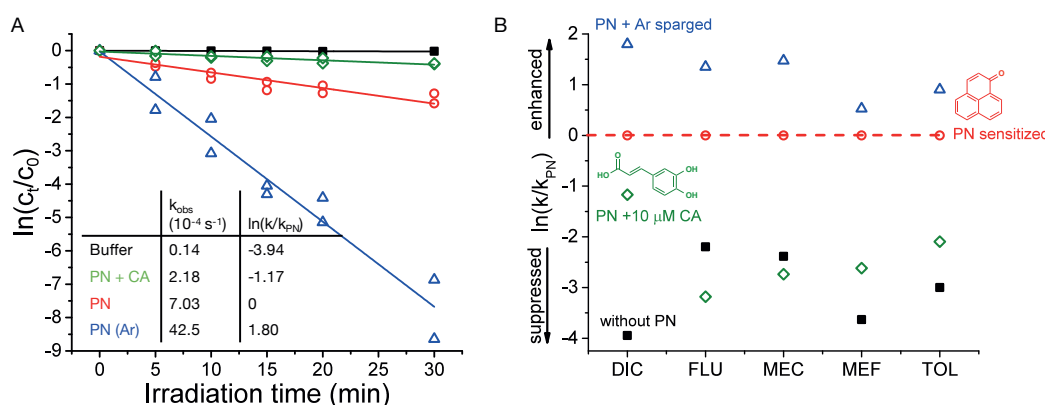


Figure 3. (A) Pseudo-first order degradation of diclofenac (5 μ M) in enhanced UVA light in phosphate buffer (pH 7.5) only: black squares (■), in the presence of the triplet sensitizer perinaphthenone (PN, 0.77 μ M, atmospheric conditions): red circles (●), with PN and anoxic (argon sparged): blue triangles (△), and with PN and the antioxidant caffeic acid (CA, 10 μ M, atmospheric conditions): green diamonds (◇). The inset shows the reaction rate constants, k_{obs} for each condition and these k_{obs} normalized by the k_{obs} obtained in presence of PN under atmospheric conditions (k_{PN}) as $\ln(k/k_{PN})$. (B) Normalized reaction rate constants, $\ln(k/k_{PN})$, for diclofenac (DIC), flufenamic acid (FLU), meclofenamic acid (MEC), mefenamic acid (MEF), and tolfenamic acid (TOL) for all conditions.

Data in Figure 3B show reaction rate constants of compounds **1-5** under different experimental conditions, each normalized to the respective rate constant obtained in the presence of PN under air saturated conditions, $\ln(k/k_{PN})$. The normalized ratio, $\ln(k/k_{PN})$, allows one to compare the effect of triplet quenchers on the overall photosensitization. The data demonstrate that anoxic conditions significantly increased the reaction rate constant by factor 3.5 to 5.7 (compared to degradation

without sensitizer). Thus, compounds **1-5** significantly react with the triplet sensitizer. The reactivity with model sensitizers further reinforces the hypothesis that triplet state DOM may account for the additional enhancement of photodegradation as observed for mefenamic acid and diclofenac. Data in Figure 3B further shows that the presence of a model antioxidant, caffeic acid, significantly quenched triplet sensitized degradation for compounds **1-5** by a factor of 1.2 to 3.2. Although caffeic acid also reacts with $^3\text{PN}^*$, we estimated that this reaction only accounts for a minor change in the steady state concentration of $^3\text{PN}^*$ (approx. 6%, Figure S6, Text S7). Flufenamic acid and meclofenamic acid show significant reactivity towards $^3\text{PN}^*$ (Figure S15-S16), yet, a net quenching effect was observed in the presence of DOM in simulated sunlight, which may be attributed to reactions with antioxidant moieties of the DOM.

We hypothesized that the sensitizer reacts with these diphenylamine-based drugs by one-electron donation forming a radical intermediate that can be reduced back to the parent compound by electron donation from an antioxidant. These hypotheses were further investigated by transient absorption spectroscopy.

Radical intermediates and electron transfer properties.

Laser flash photolysis experiments were conducted to further elucidate the reaction mechanism of diclofenac and fenamates with triplet sensitizers and antioxidants. First, the formation of radical intermediates upon reaction with the triplet sensitizer perinaphthenone, $^3\text{PN}^*$, was demonstrated.

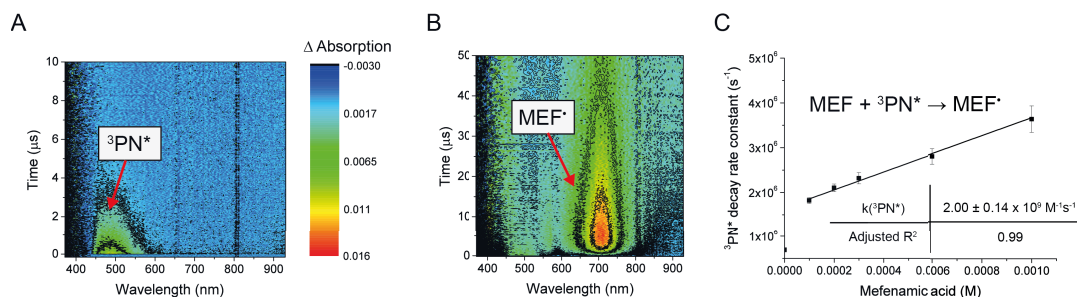


Figure 4. Three-dimensional transient absorption spectra for (A) Triplet-excited perinaphthenone ($^3\text{PN}^*$) and (B) Mefenamic acid radical (MEF^\bullet) after subtraction of scattered laser light. (C) Stern-Volmer plot showing the change in decay rate constant of $^3\text{PN}^*$ as a function of mefenamic acid concentration to determine the bimolecular reaction rate constant, $k(^3\text{PN})$. Samples were sparged with synthetic air during the experiment.

As presented in Figure 4A, $^3\text{PN}^*$ is a short lived ($1.7 \mu\text{s}$ in synthetic air) species with an absorbance centered around 479 nm. In the presence of $^3\text{PN}^*$ and mefenamic acid an additional, longer-lived transient feature appeared with approximately 300 ns delay centered around 700 nm (Figure 4B). This feature was attributed to the mefenamic acid radical. The reaction with $^3\text{PN}^*$ may proceed through an electron transfer mechanisms generating a radical cation intermediate, which deprotonates to the neutral radical. Previously, for unsubstituted diphenylamine the radical cation and neutral radical were identified with transient absorbance centered around 670 nm and 730 nm, respectively.⁴⁷ A reaction with $^3\text{PN}^*$ may also proceed through a proton coupled electron transfer (PCET).

Data in Figure 4C show the Stern-Volmer plot to determine the bimolecular reaction rate constant of $^3\text{PN}^*$ with mefenamic acid, $k(^3\text{PN}^*)$, by monitoring the decay of the $^3\text{PN}^*$ signal. The bimolecular reaction rate constants of $^3\text{PN}^*$ with compounds **1-5** were determined accordingly and range from $20 \times 10^8 \text{ M}^{-1}\text{s}^{-1}$ for mefenamic acid to $4.2 \times 10^8 \text{ M}^{-1}\text{s}^{-1}$ for diclofenac (Table 1, Figure S2-S5).

Lastly, the decelerating effect of antioxidants moieties within DOM towards the triplet reaction mechanism was investigated. Therefore, the decay rate of the radical intermediates of compound **1-4** were monitored in the presence of a model antioxidant. Here, lumichrome (LC) was used as the sensitizer because $^3\text{LC}^*$ has a higher triplet state one-electron reduction potential ($E^{\circ*} = 1.91 \text{ eV}$)⁵³ compared to $^3\text{PN}^*$ and more intense transient signals of the radical intermediates were achieved, critical to evaluate their decay rates accurately.

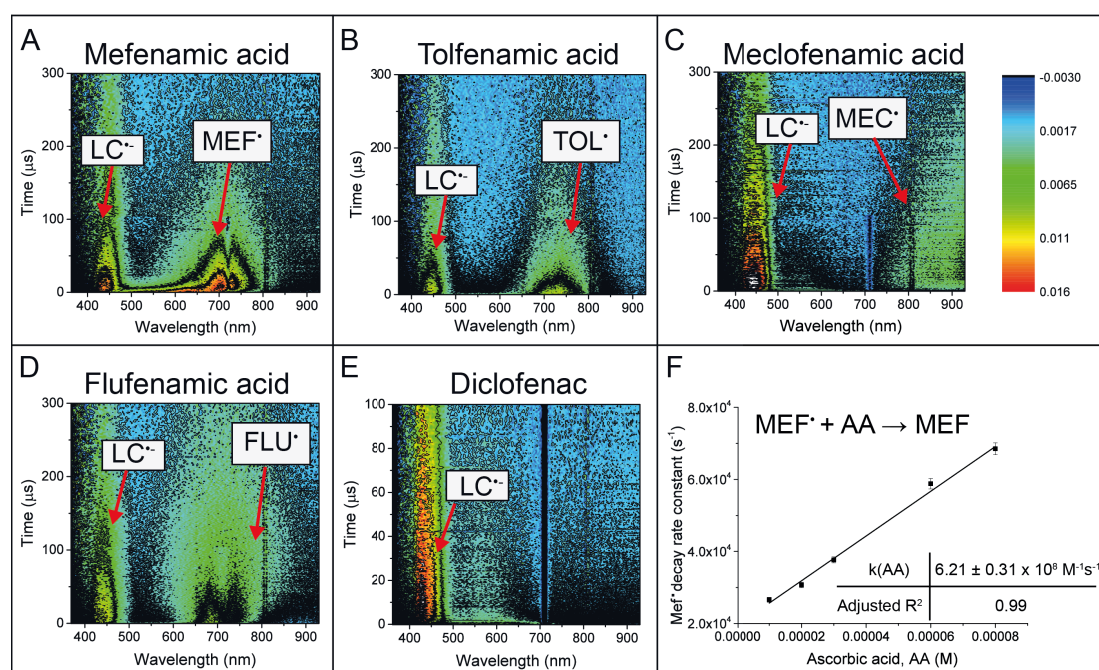


Figure 5. Transient absorption spectra for the radical intermediate formation of (A) Mefenamic acid (Mef $^{\bullet}$), (B) Tolfenamic acid (Tol $^{\bullet}$) (C) Meclofenamic acid (Mec $^{\bullet}$), (D) Flufenamic acid (Flu $^{\bullet}$). (E) No radical intermediate formation for diclofenac, but triplet lumichrome ($^3\text{LC}^*$) has reacted and strong radical anion (LC $^{\bullet-}$) is formed. Blue vertical lines at 720 nm are a result of scattered laser light. (F) Stern-Volmer plot showing the decay rate constant of the Mef $^{\bullet}$ versus the model antioxidant concentration (ascorbic acid) to determine the bimolecular reaction rate constant, $k(\text{AA})$. Samples were sparged with argon throughout the experiment.

Data in Figure 5 show the transient absorbance of the fenamate radical intermediates as they appear in the presence of $^3\text{LC}^*$. The $^3\text{LC}^*$ feature (Figure S19), centered around 630 nm, reacts fast with the fenamates and is no longer visible on the selected timescale. In addition, for the reaction with all compounds **1-5** the transient absorbance of the lumichrome radical anion, $\text{LC}^{\bullet-}$, centered around 425 nm (803 ns delay), was observed and agrees with its transient signal observed previously at a similar wavelength.⁵⁴ The simultaneous occurrence of the sensitizer radical anion and the radical intermediates of the test compounds strongly suggest that the reaction proceeds through a one electron transfer mechanism. Although the radical feature was not observed for diclofenac, the $\text{LC}^{\bullet-}$ was formed suggesting the same reaction mechanism.

Data in Figure 5F show the Stern-Volmer plot to determine the bimolecular reaction rate constants of Mef^{\bullet} with a model antioxidant, ascorbic acid $k_{(\text{AA})}$, by monitoring the change in the decay rate constant of the Mef^{\bullet} signal. The bimolecular reaction rate constants were determined accordingly for all fenamates and ranged from $62.1 \times 10^7 \text{ M}^{-1}\text{s}^{-1}$ for mefenamic acid to $3.3 \times 10^7 \text{ M}^{-1}\text{s}^{-1}$ for meclofenamic acid (Table 1, Figures S7-S9).

Based on the high reactivity of compounds **1-5** with triplet sensitizer, one would expect an overall increase in photodegradation in the presence of DOM. However, DOM (PLFA) did not show net sensitizing effects in the solar simulator towards flufenamic acid and meclofenamic acid (summary in Table S4). First, the model sensitizer perinaphthenone employed here cannot represent all different sensitizing moieties within DOM. Perinaphthenone has a relatively low triplet state one-electron reduction potential ($E^{0*} (^3\text{S}^*/\text{S}^-) = 1.03 \text{ V}_{\text{SHE}}$)⁵³ and thus can be considered a conservative model compound for DOM triplets. Secondly, the effect of DOM varies

with DOM source. Here, experiments with Suwannee River Fulvic Acid II (10 mg_C L⁻¹) in simulated sunlight resulted in similar trends but slightly different decay rates than observed with PLFA (Figure S20). In addition, the high reactivities with model antioxidants demonstrate that redox-active DOM may decelerate photodegradation of fenamates effectively. Consequently, the presence of DOM may not always show a strong net sensitizing effect. These phenomena are particularly relevant for compounds reacting via a radical intermediate, which can be reduced by antioxidant moieties present in DOM. While we have examined several possible decay pathways for the radical intermediates, other pathways, e.g., reaction with superoxide, remain untested and could be contributing to the overall degradation processes. The overall effect of DOM on the photochemical half-lives of these compounds depends on the quantity and quality of redox-active moieties and varies among DOM sources.⁵⁵

Implications

The contribution of direct photochemical degradation varies among diclofenac and the fenamates and can play a dominant role at the water surface. While all compounds showed significant reactivity towards singlet oxygen and hydroxyl radicals, these reactive oxygen species can only partially contribute to their natural attenuation in the environment. Not all compounds showed a net increase of the photodegradation rate in the presence of DOM. One electron oxidation and reduction mechanisms with sensitizing and antioxidant moieties within DOM have been positively identified by the radical intermediate detected in transient absorption spectroscopy. We demonstrate that DOM plays two roles in the photodegradation these diphenylamine-based drugs, which is similar to anilines⁵⁶, sulfonamide antibiotics⁵⁶, dimethylaniline-based drugs⁵⁷, and tryptophan⁵⁸. These compounds each

undergo oxidation by triplet excited DOM, which proceeds through a radical intermediate that can be converted back to the parent compound by a suitable electron donor, such as antioxidant moieties in DOM. In addition to DOM acting as a quencher of the fenamate radical intermediate, superoxide arising from DOM sensitization may play a similar role.⁵⁹ Consequently, the effect of DOM on the overall photodegradation rate of these compounds is dependent on the DOM's redox properties.

While the presented data show that diclofenac and the fenamates can undergo direct and indirect photochemical reactions, the half-lives are relatively long when taking into account diurnal and seasonal sunlight intensities. Where natural attenuation may not curb the concentration of these NSAIDs enough, additional measures are required to either limit their input into surface waters or to enhance water treatment for drinking water purposes. Hollender et al. demonstrated that treatment using a primary clarification and ozonation was able to completely remove both mefenamic acid and diclofenac.²⁴ Advanced oxidation technologies, such as ozonation, are however not implemented in most of the municipal wastewater treatment plants globally.⁶⁰ In general diclofenac and mefenamic acid are more widely distributed and these compounds have been included in monitoring studies more regularly. Depending on the usage pattern of these pharmaceutical, the other fenamates should also be monitored as their common mode of action (cyclooxygenase inhibition) may result in mixture toxicity effects.

Associated content.

Electronic Supplementary Information. Detailed methodology (Text S1-S7), Tables S1-S4, and Figures S1-S20. This material is available free of charge via the Internet

564 at <http://pubs.acs.org>.

565

566 **Acknowledgements.**

567 We gratefully acknowledge support of the Swiss National Science Foundation (Grant

568 number 200021-156198). We thank Ladina Birolini for her support on this project.

569

References

1. B. Nicoletti and G. Mignemi, *Minerva Med*, 1978, **69**, 3293-3297.
2. A. Raz, H. Stern and Kenigwak.R, *Israel J Med Sci*, 1973, **9**, 556-556.
3. Y. Gafni, M. Schwartzman and A. Raz, *Prostaglandins*, 1978, **15**, 759-772.
4. R. J. Flower, *Pharmacol Res Commun*, 1974, **26**, 33-67.
5. R. Menasse, P. R. Hedwall, J. Kraetz, C. Pericin, L. Riesterer, A. Sallmann, R. Ziel and R. Jaques, *Scand J Rheumatol*, 1978, 5-16.
6. R. G. Khalifah, C. E. Hignite, P. J. Pentikainen, A. Penttila and P. J. Neuvonen, *Eur J Drug Metab Ph*, 1982, **7**, 269-276.
7. P. J. Pentikainen, A. Penttila, P. J. Neuvonen, R. G. Khalifah and C. E. Hignite, *Eur J Drug Metab Ph*, 1982, **7**, 259-267.
8. J. R. Koup, E. Tucker, D. J. Thomas, A. W. Kinkel, A. J. Sedman, R. Dyer and M. Sharoky, *Biopharm Drug Dispos*, 1990, **11**, 1-15.
9. T. Reemtsma, S. Weiss, J. Mueller, M. Petrovic, S. Gonzalez, D. Barcelo, F. Ventura and T. P. Knepper, *Environmental science & technology*, 2006, **40**, 5451-5458.
10. I. Michael, L. Rizzo, C. S. McArdeell, C. M. Manaia, C. Merlin, T. Schwartz, C. Dagot and D. Fatta-Kassinos, *Water Res*, 2013, **47**, 957-995.
11. Y. L. Luo, W. S. Guo, H. H. Ngo, L. D. Nghiem, F. I. Hai, J. Zhang, S. Liang and X. C. C. Wang, *Sci Total Environ*, 2014, **473**, 619-641.
12. B. Petrie, R. Barden and B. Kasprzyk-Hordern, *Water Res*, 2015, **72**, 3-27.
13. E. L. Schymanski, H. P. Singer, P. Longree, M. Loos, M. Ruff, M. A. Stravs, C. Ripolles Vidal and J. Hollender, *Environmental science & technology*, 2014, **48**, 1811-1818.
14. L. Wang, G. G. Ying, J. L. Zhao, X. B. Yang, F. Chen, R. Tao, S. Liu and L. J. Zhou, *Sci Total Environ*, 2010, **408**, 3139-3147.
15. S. Dahane, M. D. G. Garcia, M. J. M. Bueno, A. U. Moreno, M. M. Galera and A. Derdour, *J Chromatogr A*, 2013, **1297**, 17-28.
16. T. A. Ternes, *Water Res*, 1998, **32**, 3245-3260.
17. H. B. Lee, T. E. Peart and M. L. Svoboda, *J Chromatogr A*, 2005, **1094**, 122-129.
18. M. Stumpf, T. A. Ternes, R. D. Wilken, S. V. Rodrigues and W. Baumann, *Sci Total Environ*, 1999, **225**, 135-141.

- 604 19. P. McGettigan and D. Henry, *PLoS Med*, 2013, **10**, e1001388.
- 605 20. J. L. Oaks, M. Gilbert, M. Z. Virani, R. T. Watson, C. U. Meteyer, B. A.
606 Rideout, H. L. Shivaprasad, S. Ahmed, M. J. I. Chaudhry, M. Arshad, S.
607 Mahmood, A. Ali and A. A. Khan, *Nature*, 2004, **427**, 630-633.
- 608 21. H. R. Buser, T. Poiger and M. D. Muller, *Environmental science &*
609 *technology*, 1998, **32**, 3449-3456.
- 610 22. T. Heberer, *J Hydrol*, 2002, **266**, 175-189.
- 611 23. R. Andreozzi, R. Marotta and N. Paxeus, *Chemosphere*, 2003, **50**, 1319-1330.
- 612 24. J. Hollender, S. G. Zimmermann, S. Koepke, M. Krauss, C. S. McArdell, C.
613 Ort, H. Singer, U. von Gunten and H. Siegrist, *Environmental science &*
614 *technology*, 2009, **43**, 7862-7869.
- 615 25. A. Tauxe-Wuersch, L. F. De Alencastro, D. Grandjean and J. Tarradellas,
616 *Water Res*, 2005, **39**, 1761-1772.
- 617 26. C. I. Kosma, D. A. Lambropoulou and T. A. Albanis, *Sci Total Environ*, 2014,
618 **466**, 421-438.
- 619 27. J. M. Brozinski, M. Lahti, A. Meierjohann, A. Oikari and L. Kronberg,
620 *Environmental science & technology*, 2013, **47**, 342-348.
- 621 28. C. Zwiener and F. H. Frimmel, *Sci Total Environ*, 2003, **309**, 201-211.
- 622 29. M. Carballa, G. Fink, F. Omil, J. M. Lema and T. Ternes, *Water Res*, 2008,
623 **42**, 287-295.
- 624 30. C. M. M. Hendriks, T. M. Penning, T. Z. Zang, D. Wiemuth, S. Grunder, I. A.
625 Sanhueza, F. Schoenebeck and C. Bolm, *Bioorg Med Chem Lett*, 2015, **25**,
626 4437-4440.
- 627 31. Y. Ruckebusch and P. L. Toutain, *Veterinary research communications*, 1983,
628 **7**, 359-368.
- 629 32. L. Araujo, N. Villa, N. Camargo, M. Bustos, T. Garcia and A. D. Prieto,
630 *Environ Chem Lett*, 2011, **9**, 13-18.
- 631 33. O. S. A. Al-Khazrajy and A. B. A. Boxall, *J Hazard Mater*, 2016, **317**, 198-
632 209.
- 633 34. A. Avdeef, K. J. Box, J. E. A. Comer, C. Hibbert and K. Y. Tam, *Pharmaceut*
634 *Res*, 1998, **15**, 209-215.
- 635 35. C. Giaginis and A. Tsantili-Kakoulidou, *J Liq Chromatogr R T*, 2008, **31**, 79-
636 96.
- 637 36. J. L. Packer, J. J. Werner, D. E. Latch, K. McNeill and W. A. Arnold, *Aquat*
638 *Sci*, 2003, **65**, 342-351.

- 639 37. S. Rafqah and M. Sarakha, *J Photoch Photobio A*, 2016, **316**, 1-6.
- 640 38. J. J. Werner, K. McNeill and W. A. Arnold, *Chemosphere*, 2005, **58**, 1339-
641 1346.
- 642 39. E. M. L. Janssen, E. Marron and K. McNeill, *Environ Sci-Proc Imp*, 2015, **17**,
643 939-946.
- 644 40. J. R. Laszakovits, Berg, S. M., Anderson, B. G., *Environ Sci Technol Lett*,
645 2016, DOI: 10.1021/acs.estlett.6b00422.
- 646 41. A. Leifer, <<The>> *kinetics of environmental aquatic photochemistry theory*
647 *and practice*, American Chemical Society, Washington, 1988.
- 648 42. A. L. Boreen, B. L. Edhlund, J. B. Cotner and K. McNeill, *Environmental*
649 *science & technology*, 2008, **42**, 5492-5498.
- 650 43. D. E. Latch, *Compr Ser Photoch*, 2016, **12**, 139-165.
- 651 44. G. V. Buxton, C. L. Greenstock, W. P. Helman and A. B. Ross, *J Phys Chem*
652 *Ref Data*, 1988, **17**, 513-886.
- 653 45. K. McNeill and S. Canonica, *Environ Sci Process Impacts*, 2016, DOI:
654 10.1039/c6em00408c.
- 655 46. R. Apak, K. Guclu, B. Demirata, M. Ozyurek, S. E. Celik, B. Bektasoglu, K.
656 I. Berker and D. Ozyurt, *Molecules*, 2007, **12**, 1496-1547.
- 657 47. L. J. Johnston and R. W. Redmond, *J Phys Chem A*, 1997, **101**, 4660-4665.
- 658 48. R. A. Lundeen, E. M. Janssen, C. Chu and K. McNeill, *Chimia (Aarau)*, 2014,
659 **68**, 812-817.
- 660 49. O. I. Aruoma and B. Halliwell, *Xenobiotica*, 1988, **18**, 459-470.
- 661 50. M. M. Huber, S. Canonica, G. Y. Park and U. Von Gunten, *Environmental*
662 *science & technology*, 2003, **37**, 1016-1024.
- 663 51. D. E. Latch, B. L. Stender, J. L. Packer, W. A. Arnold and K. McNeill,
664 *Environmental science & technology*, 2003, **37**, 3342-3350.
- 665 52. A. L. Boreen, W. A. Arnold and K. McNeill, *Abstr Pap Am Chem S*, 2004,
666 **228**, U637-U637.
- 667 53. K. McNeill and S. Canonica, *Environ Sci-Proc Imp*, 2016, **18**, 1381-1399.
- 668 54. H. Li, Z. Q. Jiang, Y. Pan and S. Q. Yu, *Res Chem Intermediat*, 2006, **32**,
669 695-708.
- 670 55. M. Aeschbacher, C. Graf, R. P. Schwarzenbach and M. Sander,
671 *Environmental science & technology*, 2012, **46**, 4916-4925.

- 672 56. J. Wenk and S. Canonica, *Environmental science & technology*, 2012, **46**,
673 5455-5462.
- 674 57. F. Leresche, U. von Gunten and S. Canonica, *Environmental science &*
675 *technology*, 2016, **50**, 10997-11007.
- 676 58. E. M. L. Janssen, P. R. Erickson and K. McNeill, *Environmental science &*
677 *technology*, 2014, **48**, 4916-4924.
- 678 59. Y. Y. Li, Y. H. Pan, L. S. Lian, S. W. Yan, W. H. Song and X. Yang, *Water*
679 *Res*, 2017, **109**, 266-273.
- 680 60. P. Paraskeva and N. J. D. Graham, *Water Environ Res*, 2002, **74**, 569-581.
681